Vol. 84 (1993) *ACTA PHYSICA POLONICA A* No. 6

ELECTRON SPIN ECHO ENVELOPE MODULATION ANALYSIS OF SeO_3^- RADICAL IN $(NH_4)_3H(SeO_4)_2$ SINGLE CRYSTAL

J. TRITT-GOC, J. GOSLAR, W. HILCZER, S.K. HOFFMANN AND M.A. AUGUSTYNIAK

Institute of Molecular Physics, Polish Academy of Sciences
Smoluchowskiego 17/19, 60-179 Poznań, Poland

(Received August 17, 1993)

A detailed computer analysis of the electron spin echo envelope modulations of SeO_3^- radical in a suitable orientation of $(NH_4)_3H(SeO_4)_2$ single crystal is presented. It was found that the modulations are due to a weak dipolar coupling with nitrogens and protons of the only two neighbouring NH_4 groups among the five NH_4 groups surrounding SeO_3^- center. Isotropic dipolar coupling constant is 1.7 MHz for nitrogens and 0.9 MHz for protons. It was shown that thermal reorientations of NH_4 groups observed by NMR have a negligible effect on the electron spin echo envelope modulation pattern but can be responsible for the same value of a_{iso}^H for all protons in a NH_4 group. A good fit obtained between experimental spectra and theoretical calculations assuming nondisturbed crystal geometry indicates a small damage of the crystal by X-rays during the radical center formation.

PACS numbers: 76.60.Lz, 76.30.Mi

1. Introduction

In the pulse electron spin resonance technique an electron spin echo signal is generated as a response of a spin system to a pulse sequence [1]. The echo intensity $V(t)$ decreases with characteristic time T_M being a phase memory time of the system.

When a paramagnetic center is weakly dipolar coupled to surrounding nuclei then the electron spin echo decay function $V(t)$ is modulated with nuclear spin transition frequencies. These frequencies are the same as observed in ENDOR and/or NMR experiments. After an extraction of the modulation function from $V(t)$ decay and subsequent Fourier transformation (FT) one gets an ENDOR-like spectrum. For this reason this method is known as electron spin echo envelope modulation (ESEEM) spectroscopy or FT-ESEEM spectroscopy. ESEEM was found to

be a powerful tool in studies of structural details of paramagnetic centers especially in disordered systems [2]. Recently developed two-dimensional (2D) FT-ESEEM spectroscopy gives a new and deeper insight into a structure and dynamics of molecular and biological systems [2].

The electron spin echo modulations are not always observed. In liquids the modulations are averaged out to zero by a rapid molecular tumbling. The motional averaging can also appear in solids and for this reason the modulations are sometimes not observed in crystals at room temperature but can appear at low temperatures. A modulation pattern, moreover, can be disturbed or even smeared out when a pulse sequence or a pulse timing are not chosen properly. When, however, modulations are observed one can obtain the following information:

— types of the magnetic nuclei surrounding the resonance center,
— the number and distance of the nuclei to the center,
— parameters of the hyperfine and quadrupole interactions.

Most of the papers on ESEEM deal with powders and frozen solutions (glasses). From ESEEM of such systems spatially averaged information about the resonance center environment can be deduced. For single crystals much more rich information containing anisotropic data can be obtained. However, only few papers were published on this subject [3, 4] and moreover a comparison of the anisotropic single crystal data and isotropic powder data seems to indicate some discrepancies which are not clear. It can be related to the fact that electron spin echo studies can be performed for diluted paramagnetic centers only. In condensed paramagnets with exchange and dipolar coupling between paramagnetic centers, the electron spin relaxation processes are very fast and neither a free induction decay signal nor a spin echo signal can be detected using modern pulse EPR spectrometers. For this reason the resonance centers for ESE studies are artificially introduced to the single crystals as admixture paramagnetic ions (with concentration of about 10^{18} ions/gram) or as free radicals generated by γ- or X-ray irradiation. These "defect" centers can adopt the host lattice geometry or some local lattice deformations can appear. ESEEM spectroscopy can give answer to these questions and moreover can inform on the electronic structure of the paramagnetic center i.e. on a distribution of the unpaired electron density over molecule on a molecular orbital where unpaired electron is mainly localized.

In this paper we present ESEEM studies of the SeO_3^- radicals produced by X-ray irradiation in $(NH_4)_3H(SeO_4)_2$ single crystals [5]. These radicals appear as a result of breaking of the longest Se–O bond in SeO_4^{2-} ions and the resulting unpaired electron is expected to be localized mainly on the $3p_z$ orbital of the selenium atom [6]. We will apply and test a computer algorithm for simulations of ESEEM pattern in $(NH_4)_3H(SeO_4)_2$.

Question is what are the interactions of the electron with surrounding nuclei. Is the molecular arrangement around the radical center disturbed or not, as compared to the host lattice? Does the information obtained from ESR or ESEEM of SeO_3^- radicals can be applied to the rest of unperturbed crystal and an interpretation of the molecular mechanisms of the phase transitions in the crystal? It

is well known that the NH_4 groups undergo isotropic reorientations in the crystal [7]. The question how these reorientations influence, if at all, the ESEEM pattern is still open. We will discuss this point in the paper.

2. Experimental

Paramagnetic centers in triammonium hydrogen diselenate $(NH_4)_3H(SeO_4)_2$ crystals were generated using X-ray tube Cu-K_α operating at 34 kV with 15 mA current. An approximately 1 hour irradiation results in a formation of NH_3^+ and SeO_3^- radicals as we identified by continuous wave EPR. The NH_3^+ radicals are very unstable in the crystal and vanish completely in a few minutes. The SeO_3^- radicals are a few days stable in darkness but are very sensitive to the light. An initial concentration of the SeO_3^- radicals in the crystal were estimated to be about 10^{17} spins/gram which is low enough to neglect interradical interactions in a description of pulse ESR.

Two-pulse ESE experiments were performed on a BRUKER ESP 380E FT/CW spectrometer equipped with a flow helium OXFORD CF935 cryostat. The pulse length was fixed to 16 ns with the initial interpulse interval $\tau = 144$ ns. The amplitude of pulses was adjusted to obtain the maximal spin echo amplitude. The echo signal was detected at the time 2τ as a function of the time interval τ between the first and second pulse. The measurements were performed for a fixed crystal orientation chosen according to the CW ESR measurements [5] with the external magnetic field direction in *ca* crystal plane at the angle $\Theta = 45°$. The ESR spectrum of SeO_3^- radicals in $(NH_4)_3H(SeO_4)_2$ crystals consists of a strong central line for ^{76}Se isotope (92.4% abundance) and a weak hyperfine doublet from ^{77}Se (7.5% abundance). The line width is about 0.27 mT, thus the 16 ns pulse of 2.23 mT spectral width allowed to excite the whole central line.

The ESE experiments were performed in the temperature range from 4.2 K to 300 K with measurements of spin relaxation times T_M and T_1 [8] and recording ESEEM. The best resolved ESEEM pattern was obtained at 121 K. An analysis of ESEEM observed at 121 K was performed on the basis of the room temperature structural data [9] since low temperature data are not available. Recent X-ray diffraction studies [10] indicate that there are not significant structural changes between room temperature and 120 K.

3. Theory of ESEEM analysis

To extract hyperfine and geometrical data from spin echo modulation pattern it is necessary to calculate an expected modulation pattern assuming hyperfine splitting and electron-nuclear geometry, and then to fit by a computer the theoretically predicted pattern to the experimental one.

The general approach to the ESEEM simulations based on the density matrix treatment was developed by Mims [11]. Explicit expressions for ESEEM can be obtained for any nucleus if quadrupole interaction is neglected. When the quadrupole interaction term is included in the spin Hamiltonian, the analytical expression for ESEEM can be obtained for $I = 1$ and $I = 3/2$ only. For higher spins only numerical solutions can be found [12].

The unpaired electron of the SeO_3^- radical ($S = 1/2$) in $(NH_4)_3H(SeO_4)_2$ crystal can be weakly coupled by dipolar interaction to protons ^1H ($I = 1/2$) and nitrogens ^{14}N ($I = 1$) of the neighboring NH_4^+ groups. This interaction is too weak to produce resolved hyperfine splitting in CW ESR spectrum but modulates the local magnetic field at the electron site and thus modulations of the spin echo decay function are observed.

The modulation function $V_{\mathrm{mod}}(2\tau)$ i.e. a dependence of the spin echo amplitude oscillations on the delay time 2τ between the two pulses, for the case of $S = 1/2$ and $I = 1/2$ can be written in the form

$$V_{\mathrm{mod}}(2\tau) = 1 - 2k\sin^2(\omega_\alpha\tau/2)\sin^2(\omega_\beta\tau/2), \tag{1}$$

where $k = (\omega_I B/\omega_\alpha\omega_\beta)^2$ is a modulation depth parameter and $\omega_I = g_N\mu_N B_{\mathrm{ext}}/\hbar$ is the free nuclear frequency (in rad/s) for protons in external magnetic field B_{ext} (in tesla). The frequencies (rad/s):

$$\omega_\alpha = \left[\left(\frac{A}{2}+\omega_I\right)^2 + \left(\frac{B}{2}\right)^2\right]^{1/2} \quad \text{and} \quad \omega_\beta = \left[\left(\frac{A}{2}-\omega_I\right)^2 + \left(\frac{B}{2}\right)^2\right]^{1/2}$$

are the nuclear frequencies in the lower and upper electron spin states, and A and B (in rad/s) describe the electron–nucleus dipolar coupling in point-dipole approximation

$$A = \frac{\mu_0}{4\pi\hbar}\frac{gg_N\mu_B\mu_N}{r^3}(3\cos^2\theta - 1) + 2\pi a_{\mathrm{iso}},$$
$$B = \frac{\mu_0}{4\pi\hbar}\frac{gg_N\mu_B\mu_N}{r^3}(3\cos\theta\sin\theta),$$

where g is electronic g factor and r (in meters) is the length of the electron nucleus radius r, θ is the angle between radius r and the direction of the applied field $\boldsymbol{B}_{\mathrm{ext}}$. The isotropic dipolar term a_{iso} (in rad/s) results from a delocalization of the unpaired electron on the s orbital of the atom with $I = 1/2$ nucleus.

Equation (1) can be written in the equivalent form

$$V_{\mathrm{mod}}(2\tau) = 1 - \frac{k}{4}[2 - 2\cos\omega_\alpha\tau - 2\cos\omega_\beta\tau + \cos(\omega_\alpha - \omega_\beta)\tau + \cos(\omega_\alpha + \omega_\beta)\tau]. \tag{2}$$

From Eq. (2) it is clearly seen that nuclear frequencies ω_α, ω_β and their differences and sums occur in a spin echo modulation pattern.

The modulation function resulting from interaction with ^{14}N nucleus ($I = 1$) has the form

$$V_{\mathrm{mod}}(2\tau) = 1 - \frac{16}{3}k\sin^2\left(\frac{\omega_\alpha\tau}{2}\right)\sin^2\left(\frac{\omega_\beta\tau}{2}\right) + \frac{16}{3}k^2\sin^4\left(\frac{\omega_\alpha\tau}{2}\right)\sin^4\left(\frac{\omega_\beta\tau}{2}\right). \tag{3}$$

When the spin echo amplitude modulations result from coupling to several nuclei, the expected modulation pattern can be calculated using a simple product rule

$$V_{\mathrm{mod}}^n = \prod_{i=1}^{n} V_{\mathrm{mod}}^i. \tag{4}$$

This rule holds for both identical and different nuclei and indicates that a modulation depth increases rapidly when the number of equivalent, identical nuclei increases.

As is seen from Eq. (1)–(4) for calculations of V_{mod} it is necessary to know the geometry of a disposition of the nuclei interacting with the unpaired electron (n_i, r_i) and isotropic hyperfine constant a_{iso}. In disordered system, assuming a_{iso} values one can obtain data about the above mentioned geometry. In single crystals the geometry can be known and one can obtain values of a_{iso} which describes electronic structure of the paramagnetic center.

An analysis of modulation pattern should be accompanied by an analysis of the ESEEM spectrum obtained from the Fourier transform of the experimental modulation function. These two analyses should give consistent results. The ESEEM spectrum is very sensitive to a relative number of inequivalent nuclei involved in electron nuclei interactions, and the shape or splitting of the ENDOR lines can help in an estimation of A, B or a_{iso} especially for disordered systems.

4. Results and discussion

From the set of the modulation patterns measured in our experiment we chose the one obtained at 121 K because of a good signal-to-noise ratio and well pronounced modulations. The echo decay V_{echo} is a product of decay function V_{decay} and modulation pattern V_{mod}:

$$V_{\mathrm{echo}} = V_{\mathrm{decay}} V_{\mathrm{mod}}. \tag{5}$$

The function V_{echo} for SeO_3^- radical in $(NH_4)_3H(SeO_4)_2$ single crystal in temperature 121 K is presented in Fig. 1. It is a typical spin echo decay modulated by

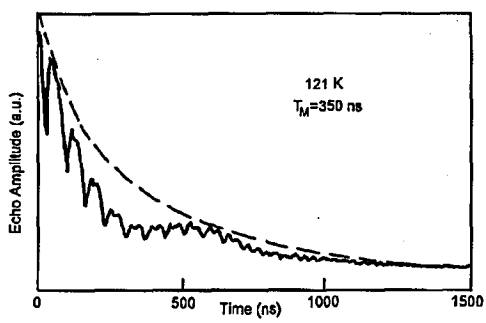

Fig. 1. Two-pulse electron spin echo amplitude decay for SeO_3^- radical in $(NH_4)_3H(SeO_4)_2$ at 121 K. The dashed line is an exponential phase relaxation $V_{\mathrm{dec}} = V_0 \exp(-2\tau/T_{\mathrm{M}})$ with phase memory time $T_{\mathrm{M}} = 350$ ns in absence of modulations.

at least three frequencies. To analyze the V_{mod} function it is necessary to subtract V_{decay} from V_{echo} in some way. The most widely used method is to make a computer fit of monoexponential function in such a way that the decay function is

lead through modulation maxima (dashed curve in Fig. 1). This monoexponential decay function is described by an equation

$$V_{\text{decay}} = \exp(-2\tau/T_{\text{M}}) \tag{6}$$

with T_{M} being phase memory time. For our pattern at 121 K, $T_{\text{M}} = 350$ ns. In order to get the pure modulation pattern we subtracted V_{decay} from V_{echo} and the result is presented in Fig. 2a. The Fourier transform of the modulation pattern

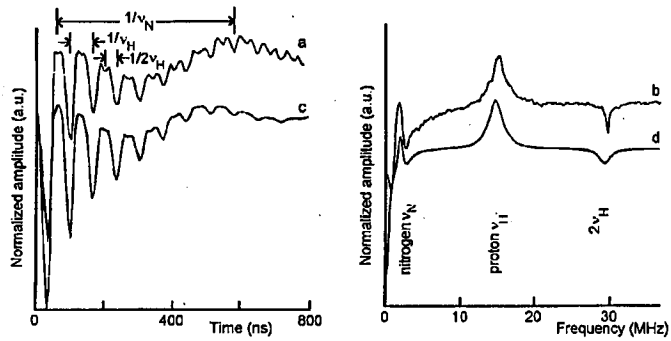

Fig. 2. Experimental (a) and simulated (c) two-pulse ($\tau = 144$ ns) ESEEM patterns at 121 K of SeO_3^- radical in $(NH_4)_3H(SeO_4)_2$ single crystal. The fit parameters are given in the text. Parts (b) and (d) are the corresponding FT spectra.

presented in Fig. 2a gives an ESEEM spectrum shown in Fig. 2b. The line at 14.6 MHz and phase-reversed line at 29.2 MHz are fundamental and first harmonic proton frequencies, respectively. The similar doublet clearly seen at low frequencies can be ascribed to nitrogen ^{14}N frequencies with 1.05 MHz as the fundamental frequency. Thus we can conclude that the modulations of the electron spin echo decay observed in our experiment are due to protons and nitrogens from NH_4 groups surrounding the SeO_3^- radical. Moreover, we can also conclude that these nuclei are weakly coupled to paramagnetic center ($r > 0.3$ nm) because otherwise the ESEEM spectrum should contain not only the ENDOR frequencies ω_α, ω_β but also their sum and difference frequencies.

To extract information about the proton and nitrogen hyperfine coupling constants and the number of interacting nuclei we have to perform detailed analysis of the modulation pattern. To do this one has to calculate theoretical ESEEM spectrum and find the best fit to experimental one. We used expressions (1)–(3) to simulate theoretical ESEEM spectra. It is worth pointing out that we used simplified Eq. (3) for modulations resulting from $I = 1$ nuclei. This equation is valid when the quadrupole term for ^{14}N is small as compared with the Zeeman energy. An analysis of published data demonstrates that this condition is violated for ^{14}N because the quadrupole coupling constant is either comparable or even exceeds the nuclear Zeeman coupling. However, this approximation can be used in X-band EPR experiments that involve coupling with ^{14}N nuclei in environments that minimize the effect of nuclear quadrupole coupling. This is the situation for nitrogen in NH_4 group.

A detailed analysis of the modulation pattern was performed according to Eq. (4) inserting Eqs. (2) and (3) and using as an input data $B_{ext} = 343$ mT, $\omega_{proton} = 14.6$ MHz, $\omega_{nitrogen} = 1.05$ MHz and neglecting nitrogen quadrupole interaction for the reasons mentioned above. We took into account the real geometric arrangement of protons and nitrogens around SeO_3^- paramagnetic center known from crystallographic data for room temperature [9]. This is presented in Fig. 3. The SeO_3^- radical with the single unpaired electron located mainly on p_z

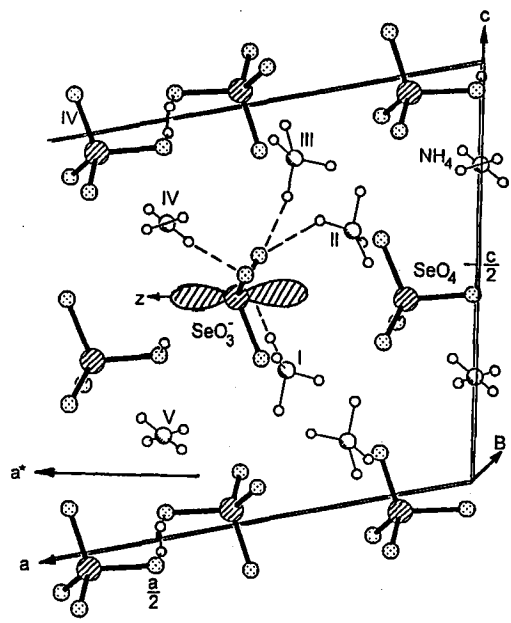

Fig. 3. Projection of the $(NH_4)_3H(SeO_4)_2$ structure along b axis. The p_z orbital of SeO_3^- radical is drawn. Dotted lines represent hydrogen bonds between selenate group and the nearest NH_4 groups. The direction of the external magnetic field B for which the ESEEM was recorded is marked.

orbital of Se atom is surrounded by five NH_4 groups marked as I–V in Fig. 3. The I–IV groups are linked by hydrogen bonds (dashed lines in Fig. 3) with SeO_3^- and their nitrogen atoms are at distances from the Se atom: 0.369, 0.377, 0.379, and 0.399 nm respectively. The V group which is located only at slightly longer distance is not hydrogen bonded to the selenate group, thus only anisotropic dipolar contribution to hyperfine coupling is expected without an isotropic contribution from unpaired electron density delocalization. The only parameters which were changing in order to obtain the best fit between theoretical and experimental pattern were the number of interacting protons and nitrogens and hyperfine coupling constant for these nuclei.

In order to illustrate how different parameters influence the ESEEM pattern we calculated two-pulse ESEEM patterns for few sets of parameters. The effect of

the angle θ between external field and the radius r on the system containing only one hydrogen nucleus is illustrated in Figs. 4a and 5a. The angle θ affects both the

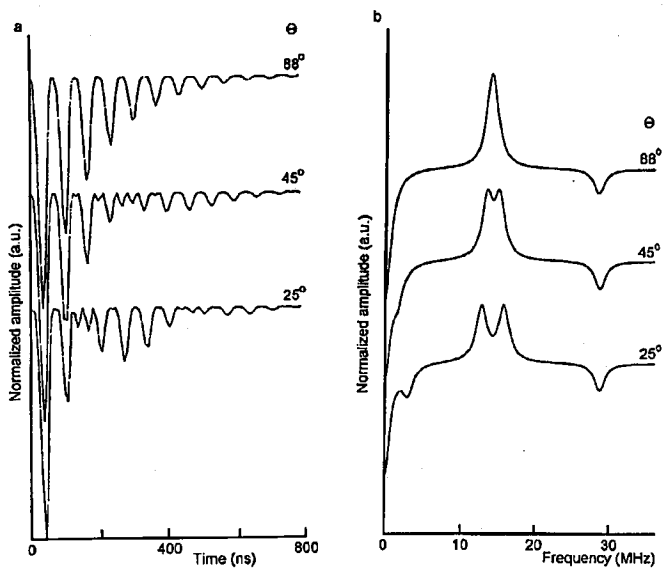

Fig. 4. Theoretical two-pulse ESEEM for a single proton showing an effect of the θ angle on the modulation pattern (a) and corresponding ESEEM spectra (b). θ is an angle between magnetic field direction and Se–H direction. The used parameters are $r = 0.38$ nm, $a_{iso} = 0.0$ MHz.

$2\omega_I$ indentation and the modulation depth. Note that most of the differences occur at interpulse distances greater than 200 ns. Figures 4b and 5b present the Fourier transforms of modulation patterns presented in Figs. 4a and 5a respectively. They show the ESEEM spectrum for protons. Comparing Figs. 4 and 5, one can recognize the effect of a_{iso} on the modulation pattern. Moreover, it is clearly seen that a modulation pattern and ESEEM spectrum are very sensitive to the geometry and isotropic dipolar coupling.

All the above simulations were performed for $r = 0.38$ nm which is typical of our crystal. At this distance the ω_I frequency dominates in the modulation but also some $2\omega_I$ contribution is apparent. Figure 6 shows the two-pulse ESEEM calculated for four protons and one nitrogen from the NH_4 group located in the nearest distance to the SeO_3^- radical in $(NH_4)_3H(SeO_4)_2$ single crystal (group I in Fig. 3). Note the deep modulation due to nitrogen in Fig. 6a and the existence of nitrogen frequencies in Fig. 6b when comparing with the spectra in Figs. 4b and 5b. These calculations were performed for real distribution of protons and nitrogen known from crystallographic data. Each hydrogen has its own angle θ and distance r but the common a_{iso} value (see Fig. 6).

From our ^1H NMR spin–lattice measurements [7] we know that the protons from NH_4^+ groups in triammonium hydrogen diselenate crystals undergo a rapid

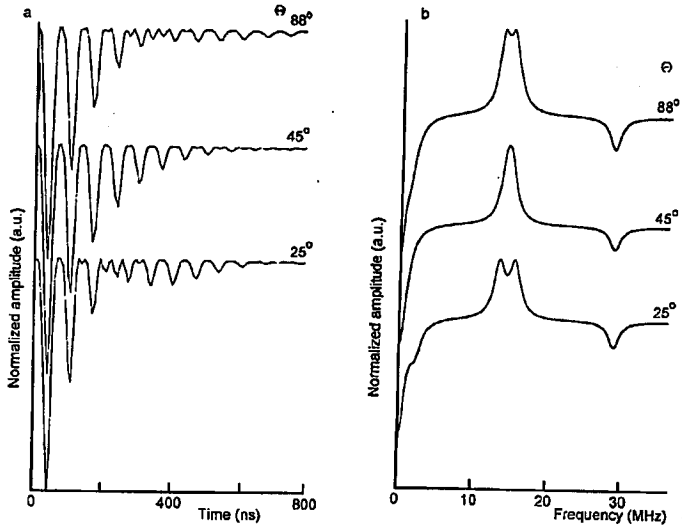

Fig. 5. Theoretical ESEEM pattern plots like in Fig. 4 with $a_{iso} = 1.0$ MHz.

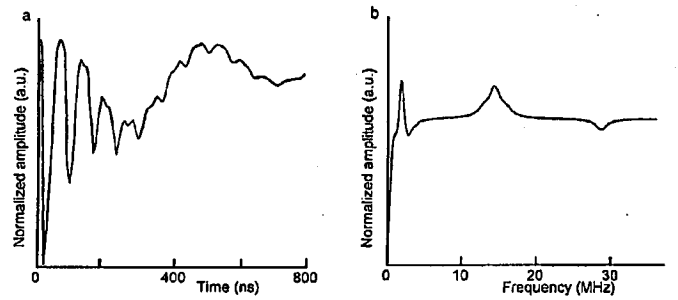

Fig. 6. Calculated two-pulse ESEEM pattern for a single NH_4 group (group I) (a) and corresponding ESEEM spectrum (b). The used parameters are: ^{14}N — $r = 0.369$ nm, $\theta = 94.16°$, $a_{iso} = 1.6$ MHz; ^1H — $r_1 = 0.399$ nm, $\theta = 105.47°$, $r_2 = 0.271$ nm, $\theta = 86.70°$, $r_3 = 0.419$ nm, $\theta = 86.48°$, $r_4 = 0.401$ nm, $\theta = 94.40°$, $a_{iso} = 1.0$ MHz.

thermal motion and they can be considered to occupy their time averaged positions. For a general ionic reorientations which take place in the $(NH_4)_3H(SeO_4)_2$ single crystal this reduces to placing the NH_4 protons at the associated nitrogen site [13]. This procedure is used for example in calculating acid proton contribution to the NMR second moment. Figure 7a shows the two-pulse ESEEM for four protons placed at the associated nitrogen site. For comparison in Fig. 7b we present the modulation pattern for the same protons but placed at appropriate distances r

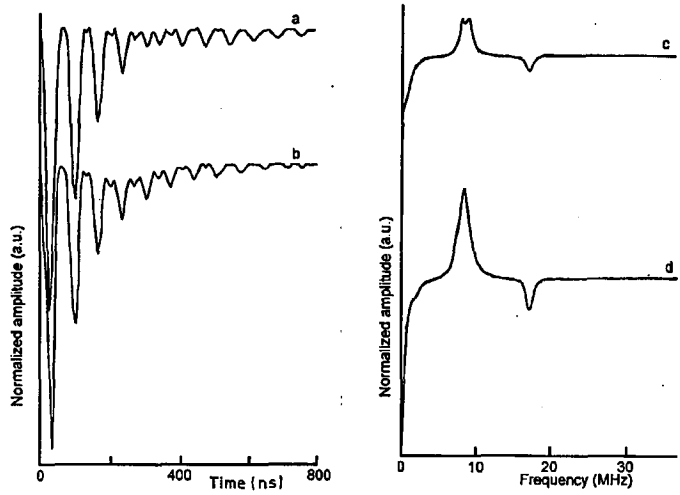

Fig. 7. Calculated two-pulse ESEEM (left figure) with corresponding Fourier transform spectra (right figure) for single I-NH_4 group: *a* — assuming averaged proton positions at the nitrogen site: $r = 0.369$ nm, $\theta = 94.16°$, $a_{iso} = 0$; *b* — taking hydrogen positions from crystallographic data with r and θ as in Fig. 6 and $a_{iso} = 0$.

at angles θ. Note a big difference between both patterns. The modulation pattern in Fig. 7b is more like the experimental one presented in Fig. 2a. Thus we decided that the model with motional averaging of the proton positions is not satisfying in our case.

It seems more reasonable to take into account the all five NH_4 groups surrounding SeO_3^- center. We have found, however, that the resulting ESEEM pattern is far from the experimental one and has bad-resolved modulations. Reducing number of interacting ammonium groups we obtained the best and satisfying fit when only group I and II were considered with $r_I = 0.369$ nm and $r_{II} = 0.376$ nm, assuming $a^H_{iso} = 0.9$ MHz for all protons and $a^N_{iso} = 1.7$ MHz for the two nitrogens. This best fit is (Fig. 2c, d) compared with experimental ESEEM pattern in Fig. 2. The fit criterion was based on the first several modulation cycles since approximation in the theory tends to cause larger deviations at longer times [12]. The fit for larger number of protons leads to a smearing out of the nitrogen modulation. For $a^H_{iso} < 0.9$ MHz the modulation depth becomes too low for the long time ($t > 400$ ns in Fig. 2a). If, however, $a^H_{iso} > 1$ MHz is assumed, the modulation due to $2\omega_H$ begins to diminish and the simulated modulation pattern becomes to be quite different from the experimental one. Thus the best fit is for $a^H_{iso} = 0.9 \pm 0.1$ MHz.

5. Conclusions

An analysis of the ESEEM spectrum of SeO_3^- radical in $(NH_4)_3H(SeO_4)_2$ single crystal showed that it is possible to fit the modulation pattern assuming nonperturbed crystal structure. It means that the X-ray radiation damage during

a SeO_3^- radical formation relaxes relatively quickly and the molecular structure and molecular arrangement is practically not disturbed. This conclusion is supported by our extended theoretical ESEEM simulations with different sets of parameters which showed that a modulation pattern is very sensitive to the radical environment geometry.

In the magnetic field orientation we used in our ESE experiments ESEEM can be fit as arising from the nitrogens and protons of the nearest two NH_4 groups with isotropic dipolar coupling constant $a_{iso}^{N} = 1.7$ MHz for nitrogens and $a_{iso}^{H} = 0.9$ MHz for protons. We did not find a distinct influence of the NH_4 group reorientations on the ESEEM spectrum. However, the reorientations can be responsible for the same a_{iso} value for all protons.

References

[1] K.M. Salikhov, A.G. Semenov, Yu.D. Tsvetkov, *Electron Spin Echoes and Their Applications*, Nauka, Novosibirsk 1976 (in Russian).

[2] L. Kevan, M.K. Bowman, *Modern Pulsed and Continuous Wave Electron Spin Resonance*, Wiley, New York 1990, Chs. 1–5.

[3] J. Isoya, M.K. Bowman, J.R. Norris, J.A. Weil, *J. Chem. Phys.* **78**, 1735 (1983).

[4] M.J. Colaneri, J.A. Potenza, H.J. Schugar, J. Peisach, *J. Am. Chem. Soc.* **112**, 9451 (1990).

[5] M.A. Augustyniak, S.K. Hoffmann, *Ferroelectrics* **132**, 129 (1992).

[6] M.A. Augustyniak, S.K. Hoffmann, J.Goslar, W. Hilczer, J. Wolak, *Ferroelectrics Lett.* **15**, 69 (1993).

[7] J. Tritt-Goc, N. Piślewski, S.K. Hoffmann, M.A. Augustyniak, *Phys. Status Solidi B* **176**, K13 (1993).

[8] W. Hilczer, S.K. Hoffmann, J. Goslar, J. Tritt-Goc, M. Augustyniak, *Solid State Commun.* **85**, 585 (1993).

[9] A. Pietraszko, K. Łukaszewicz, M.A. Augustyniak, *Acta Crystallogr. C* **48**, 2069 (1992).

[10] K. Łukaszewicz, A. Pietraszko, private communication.

[11] W.B. Mims, *Phys. Rev. B* **5**, 2409 (1972); *Phys. Rev. B* **6**, 3543 (1972).

[12] L. Kevan, in: *Time Domain Electron Spin Resonance*, Eds. L. Kevan, R.N. Schwartz, Wiley, New York 1979, Ch. 8.

[13] A. Watton, E.C. Reynhardt, H.E. Petch, *J. Chem. Phys.* **65**, 4370 (1976).